Cancer Letters 554 (2023) 216024

Contents lists available at ScienceDirect

Cancer Letters

journal homepage: www.elsevier.com/locate/canlet

An anti-EGFR antibody-drug conjugate overcomes resistance to HER2-targeted drugs

Lucía Gandullo-Sánchez, Atanasio Pandiella *

Universidad de Salamanca. Instituto de Biología Molecular y Celular del Cáncer, CSIC, IBSAL and CIBERONC, Salamanca, Spain

ARTICLE INFO

Keywords:
HER2
EGFR
Breast cancer
Drug resistance
Antibody-drug conjugate

ABSTRACT

Trastuzumab-emtansine (T-DM1) is an antibody-drug conjugate (ADC) that was approved in 2013 to treat HER2+ breast cancer. Despite its efficacy in the clinic, some patients exhibit intrinsic or acquired resistance to such ADC. To characterize mechanisms of resistance to T-DM1, we isolated several HER2+ resistant clones derived from the HCC1954 HER2+ cell line. The isolated clones were different as per their transcriptomic profiles. However, all the T-DM1-resistant clones showed decreased HER2 levels. Yet, the clones were still oncogenically dependent on HER2, as indicated by knock down experiments. The decrease in HER2 expression caused acquired resistance to T-DM1 and to other anti-HER2 therapies. Antibody array analyses showed that the epidermal growth factor receptor (EGFR) was expressed in these T-DM1-resistant HCC1954 clones. Indeed, therapies targeting EGFR, particularly cetuximab-DM1, demonstrated a strong anti-proliferative action on cells with acquired resistance to T-DM1 and HER2 loss. The expression of EGFR in cells resistant to T-DM1 offers the possibility of using therapies directed to this receptor to combat resistance to anti-HER2 drugs and loss of HER2 overexpression.

1. Introduction

ERBB2 gene amplification and overexpression occurs in approximately 20% of breast cancers and is associated with more aggressive disease [1,2]. Less frequent molecular alterations such as somatic mutations in *ERBB2* are present in approximately 4% of breast cancer patients and occur mainly in the intracellular tyrosine kinase domain or the extracellular region [3]. The correlation between HER2 overexpression and patient outcome [2], together with preclinical data corroborating a pro-oncogenic role for HER2 [4], promoted the development of agents that act specifically on this tyrosine kinase, and that have markedly improved the survival of patients with HER2 positive (HER2+) breast cancer [5,6].

Two types of anti-HER2 agents have reached the oncology clinic. On one hand, antibodies and antibody-drug conjugates (ADCs) such as pertuzumab [7,8], trastuzumab [9,10], margetuximab [11,12], trastuzumab-emtansine (T-DM1) [13,14] and trastuzumab-deruxtecan (T-DXd) [15–17]. The second group of agents that target HER2 are small molecule tyrosine kinase inhibitors (TKIs) such as lapatinib [18,19], neratinib [20–22] and tucatinib [23,24]. Despite many advances made in the early detection and adjuvant treatment of breast cancer in recent decades, a significant proportion of breast cancer patients continue developing recurrent or metastatic disease, as well as resistance to the targeted therapies [25]. Indeed, breast cancer was the most frequently diagnosed cancer worldwide for both genders in 2020 [26].

T-DM1 is composed of trastuzumab linked via a lysine residue to a noncleavable thioether linker called 4-(N-maleimidomethyl) cyclohexane-1-carboxylate (MCC) covalently bond to the maytansinoid derivative DM1, a potent inhibitor of microtubule polymerization [27]. After its approval in 2013 by the FDA, T-DM1 has become the standard second-line treatment in patients with advanced HER2+ breast cancer, who previously received trastuzumab and a taxane, separately or in combination [13]. Recently, thanks to the results of the KATHERINE clinical trial, the use of T-DM1 has been approved to treat patients with early HER2+ breast cancer who have residual invasive disease after neoadjuvant treatment based on HER2-targeted therapy and taxane [14]. Although T-DM1 has demonstrated its efficacy, some patients do not respond or the disease initially responds but relapses over time [28]. Because of that, novel strategies to overcome resistance to this drug are required [29]. In fact, recent approvals of drugs such as T-DXd, that demonstrated efficacy in the T-DM1-resistant scenario, show the clinical need of novel strategies aimed at increasing the therapeutic armamentarium against HER2+ tumors. Taking this into account, we have

* Corresponding author. Universidad de Salamanca. Instituto de Biología Molecular y Celular del Cáncer, Campus Miguel de Unamuno, 37007, Salamanca, Spain.
E-mail address: atanasio@usal.es (A. Pandiella).

https://doi.org/10.1016/j.canlet.2022.216024
Received 12 September 2022; Received in revised form 2 November 2022; Accepted 22 November 2022
Available online 29 November 2022

Abbreviations

ADC	antibody-drug conjugate
BCA	bicinchoninic acid
CANX	calnexin
Cy	cyanine
DEGs	differentially expressed genes
DMEM	Dulbecco's Modified Eagle's Medium
EGFR	epidermal growth factor receptor
FBS	fetal bovine serum
HCC-TDM1R#	HCC1954 T-DM1R clone
HER2+	HER2 positive
HRP	horseradish peroxidase
IF	immunofluorescence
IgG	immunoglobulin G
IP	immunoprecipitation
KRH	Krebs-Ringer-HEPES buffer
MCC	4-(N-maleimidomethyl) cyclohexane-1-carboxylate
PBS	phosphate-buffered saline
PCA	principal component analyses
PI	propidium iodide
PVDF	polyvinylidene difluoride
qPCR	quantitative PCR
RQ	relative quantification
RTKs	receptor tyrosine kinases
shRNA	short hairpin RNA
STR	short tandem repeat
TAC	Transcriptome Analysis Console
TBST	Tris-buffered saline with Tween
T-DM1	trastuzumab-emtansine
T-DXd	trastuzumab-deruxtecan
TKIs	tyrosine kinase inhibitors
WB	Western blot

generated T-DM1-resistant models derived from the HCC1954 HER2+ breast cancer cell line with the purpose of identifying novel therapeutic vulnerabilities to fight resistance raised against T-DM1. Genomic as well as biochemical studies demonstrated loss of HER2 in the resistant clones. Those clones were also resistant to other anti-HER2 therapies but showed sensitivity to anti-EGFR therapies, especially to a novel ADC constructed against EGFR that was based in the coupling of cetuximab to DM1.

2. Materials and methods

2.1. Reagent and immunochemicals

Generic chemicals routinely used in the laboratory were from Sigma-Aldrich (Madrid, Spain), Roche Biochemicals (St Louis, United States) or Merck (Darmstadt, Germany). Culture media, antibiotics, trypsin-EDTA, and fetal bovine serum (FBS) were purchased from Thermo Fisher Scientific (Waltham, United States). Sterile plastic material from BD Biosciences (Franklin Lakes, NJ, USA) and Corning Incorporated (Corning, New York, USA) were also purchased from Thermo Fisher Scientific. Erlotinib and gefitinib were from LC Laboratories. Lapatinib and neratinib were from Selleckchem (Houston, TX). Trastuzumab and T-DM1 were purchased from a local pharmacy (Farmacia Escudero, Salamanca, Spain) and cetuximab and T-DXd from Meritxell pharmacy (Andorra). Pertuzumab was a gift of the Oncology Service of the Avila Hospital. The remaining of the antibodies used are detailed in Supplementary Table 1 (primary antibodies) and Supplementary Table 2 (secondary antibodies). All the antibodies generated in our laboratory are rabbit polyclonal antibodies and were generated as described before [30].

The conjugation of cetuximab to SMCC-DM1 was carried out using the product HY-101070/CS-6309 from MedChemExpress (Junction, New Jersey, United States) following the manufacturer's instructions. The buffer in which cetuximab was dissolved was changed to conjugation buffer 1 (50 mM KH_2PO_4; 50 mM NaCl; 2 mM EDTA, pH 6.5), using an Amicon® Ultra-0.5 100K filter (Millipore). Cetuximab was then measured on a NanoDrop™ apparatus (Thermo Fisher Scientific) and adjusted to 20 mg/ml. The SMCC-DM1 reagent was dissolved in dimethylacetamide (DMA) at a concentration of 10 mM and a 7 molar equivalent of reagent was incubated with the antibody solution. Extra DMA was added to the conjugation solution to obtain a 10% v/v final volume of DMA. The reaction was mixed and incubated overnight at room temperature. Then, conjugation buffer 2 (50 mM sodium succinate; pH 5) was added and transferred to a Amicon® Ultra-0.5 100K filter. A total of 4 washes were performed with such buffer. Finally, the ADC solution was sterilized by filtration with a 0.22 μm low adsorption nitrocellulose filter (Millipore) and quantified in the NanoDrop™.

2.2. Cell culture and generation of resistant cell models

The HCC1954 cell line was obtained from the ATCC and cultured in Dulbecco's Modified Eagle's Medium (DMEM) supplemented with 10% FBS and antibiotics (penicillin 100 U/ml, streptomycin 100 μg/ml). All cell lines were cultured at 37 °C in a humidified atmosphere in the presence of 5% CO_2. Cell line authentication was performed by short tandem repeat (STR) at the Hematology Service of the Salamanca University Hospital.

HCC1954 cells (20,000) were plated in 150 mm dishes and treated with 1 nM T-DM1 (media replaced weekly) following a continuous treatment protocol [31]. Resistant HCC1954 T-DM1R clones (HCC-TDM1R#) were obtained by single-cell cloning and continuously cultured in the presence of 1 nM T-DM1 for a total period of 5 months. The resistant phenotype was routinely tested by cell counting.

2.3. Transfections and viral infections

For cell transfections, jetPEI® from Polyplus Transfection (Illkirch, France) and lentiviral vectors supplied by Cultek (Madrid, Spain), Addgene (Cambridge, MA, USA) or Sigma-Aldrich were used. The specific sequences are described in Supplementary Table 3. pHAGE-ERBB2 was a gift from Gordon Mills & Kenneth Scott (Addgene plasmid #116734; http://n2t.net/addgene:116734; RRID: Addgene_116734). The puromycin used for the selection was from Sigma-Aldrich (2 μg/ml for HCC1954 cells and resistant clones). Knockdowns of EGFR and HER2 and overexpression of HER2 were performed by infection with lentiviral particles as described previously [32].

2.4. Microarray analyses of mRNA and qPCR

Total RNA extraction was performed with the RNeasy Mini kit (Qiagen, Hilden, Germany) following the manufacturer's instructions. Once the RNA was obtained, the RNA concentration was determined on a NanoDrop™ 1000 (Thermo Fisher Scientific). For microarray experiments, RNA purification, integrity and cDNA synthesis were carried out by the Genomics Service of our Institute. cDNA was hybridized to Clariom S arrays human (Affymetrix, Santa Clara, USA). Raw CEL files were normalized using the RMA algorithm and the genes that presented differential expression were identified using the Transcriptome Analysis Console (TAC) software version 4.0.2.15 (Affymetrix). Cut-off for differentially expressed genes was fold change <-2 or >2 and a p-value of ANOVA <0.05.

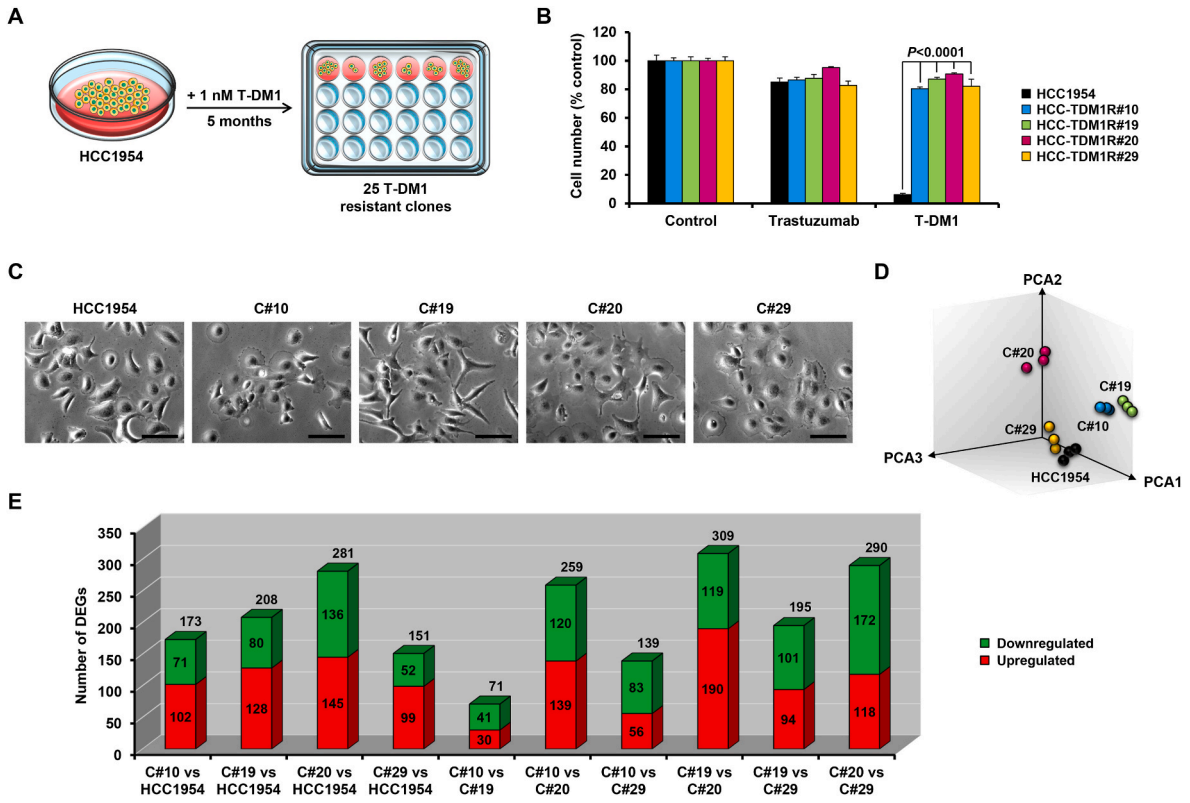

Fig. 1. Models of secondary resistance to T-DM1 generated from cells primarily resistant to trastuzumab. (A) Graphical representation of the generation of T-DM1-resistant clones from the cell line HCC1954. (B) Five-day response to trastuzumab (50 nM) and T-DM1 (1 nM) of the HCC1954 cell line and HCC-TDM1R clones. Data represent mean +SD of triplicates (normalized to untreated controls) from an experiment that was repeated at least twice. Statistics indicate the *p*-values with respect to naïve HCC1954 treated with T-DM1. (C) Phase contrast images of HCC1954 and T-DM1-resistant cells taken at × 20 magnification. Scale bar, 100 μm. (D) Principal component analysis (PCA) of data obtained from RNA microarrays from the HCC1954 cell line and T-DM1-resistant clones. (E) Number of differentially expressed genes (DEGs) among T-DM1-resistant and parental cell lines. Total DEGs for each comparison are indicated above the bar.

For qPCR performance, 2 μg of total RNA was reverse-transcribed using M-MLV Reverse Transcriptase, oligodT primers (Invitrogen, Carlsbad) and dNTPs (Fermentas Life Sciences, Burlington, Canada) in a thermocycler GeneAmp PCR System 2400 (PerkinElmer, Waltham, USA) following the instructions from the manufacturer. The cDNAs were then subjected to quantitative PCR (qPCR) analysis using SYBR® Select Master Mix for CFX (Applied Biosystems, Foster City, USA) in Applied Biosystems™ QuantStudio 1 package (Applied Biosystems, Foster City, USA). Each sample was analyzed in duplicate in 96-well optical plates on an iCycler® iQ™5 thermal cycler (Bio-Rad Laboratories). An initial step was performed at 95 °C for 5 min, followed by 40 cycles of 95 °C for 30 s, 60 °C for 30 s and finished by 72 °C for 30 s. A final melt curve stage was composed by a step of 95 °C for 1 min, a 55 °C step for 10 s and a final step of 72 °C for 10 min. The relative expression of each gene was determined using *GAPDH* as housekeeping gene. The results are presented as the relative quantification (RQ) value of each sample with respect to the HCC1954 cell line with a positive error value of maximum RQ minus RQ (RQmax-RQ) and a negative error value of RQ minus RQ minimum (RQ-RQmin). Primer sequences (Supplementary Table 4) used were designed with Primer3 software and purchased from Thermo Fisher Scientific.

2.5. Cell proliferation, cell cycle, and apoptosis analyses

Cell proliferation was analyzed by cell counting assays [33]. Briefly, cells were seeded in 6-well plates and allowed to attach overnight in DMEM. Then, the medium was replaced with complete medium containing the chosen drugs. The day of the analysis, cells were detached with trypsin-EDTA, diluted in ISOTON® (Beckman Coulter Life Sciences) and counted using a Z1 Coulter Particle Counter (Beckman Coulter, Pasadena, CA, USA). In proliferation experiments, each condition was analyzed in triplicate and data were presented as mean +SD of a representative experiment that was repeated at least twice. GraphPadPrism 8.0.2 (GraphPad Software, La Jolla, CA, USA) was used to determine IC_{50} values.

For cell cycle and apoptosis analyses cells were seeded in 6-well plates and, after 24h, were treated with desired drugs. At the indicated times, non-attached and attached cells were collected. Both assays were performed as described [32,33]. Cells were acquired using an Accuri C6 Flow Cytometer (BD Biosciences). Typically, 50,000 events were collected and analyzed using the C6 software.

2.6. Western blot and antibody arrays

Protein extraction, immunoprecipitation and Western blot protocols have been described [32,34,35]. Briefly, to prepare cell lysates, cultured cells were washed with phosphate-buffered saline (PBS) and lysed in ice-cold lysis buffer (20 mM Tris–HCl pH 7.0, 140 mM NaCl, 50 mM EDTA, 10% glycerol, 1% Nonidet P-40, 1 μM pepstatin, 1 μg/ml aprotinin, 1 μg/ml leupeptin, 25 mM β-glycerol phosphate, 50 mM sodium fluoride, 1 mM phenylmethyl sulfonyl fluoride, 1 mM sodium orthovanadate). Lysates were centrifuged at 17,000 g at 4 °C for 10 min and supernatants were transferred to new tubes. Protein concentration was determined by bicinchoninic acid (BCA) assay (Pierce™ BCA protein assay kit, Thermo Fisher Scientific). For immunoprecipitation, equal amounts of protein were incubated with protein A-Sepharose (GE Healthcare, Little Chalfont, UK) and the necessary antibody (Supplementary Table 1) for at least 2 h at 4 °C. Immune complexes were recovered by a short centrifugation at 17,000 g for 30 s and washed three times with 1 ml cold lysis buffer. Then, samples were boiled in

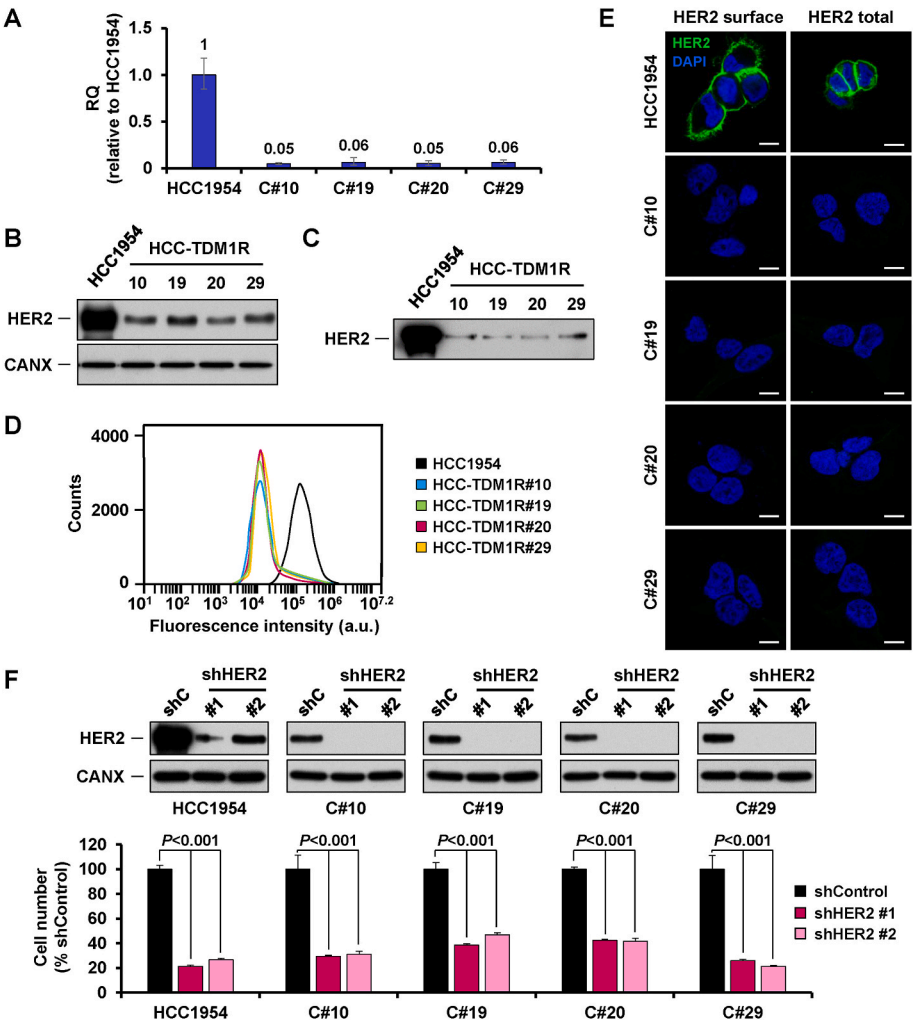

Fig. 2. T-DM1-resistant clones express low HER2 levels but remain addicted to HER2. (A) Quantitative PCR analysis of *ERBB2* mRNA levels is represented as relative quantification (RQ) in arbitrary units with respect to the value of the HCC1954 cell line and normalized with respect to *GAPDH* expression. The data is represented as the value of RQ + (RQmax-RQ) - (RQ-RQmin). (B) Total HER2 levels in parental and T-DM1-resistant cells analyzed by immunoprecipitation and Western blot. (C and D) Cell-surface HER2 level was quantitatively analyzed by surface immunoprecipitation (C) or by flow cytometry (D), using T-DM1 as primary antibody in both cases. (E) HER2 levels analyzed by immunofluorescence. Cells were fixed and stained for HER2 using trastuzumab. Scale bar, 10 μm. HER2: green, DAPI: blue. (F) Knockdown of HER2 in parental and T-DM1-resistant cell lines. Cells were infected with lentivirus containing the shRNA control (shC, shControl) or the shRNA sequences targeting HER2 (shHER2 #1 y shHER2 #2). HER2 and calnexin (CANX) levels were analyzed by western (top). The effect of HER2 knockdown (bottom) on the cell proliferation was analyzed by cell counting after 5 days. Data (normalized to control values) represent mean +SD of triplicates of an experiment that was repeated at least twice. Statistics indicate the *p*-values with respect to cells infected with shControl.

electrophoresis sample buffer and placed on SDS-PAGE gels. After electrophoresis, proteins in the gel were transferred to polyvinylidene difluoride (PVDF) membranes (Millipore Corporation, Bedford, MA, USA). Membranes were blocked in Tris-buffered saline with Tween (TBST, 20 mM Tris pH 7.5, 150 mM NaCl, 0.1% Tween 20) containing 1% BSA for at least 1 h and then incubated with the corresponding primary antibody (Supplementary Table 1) for 2 h or overnight. After three washes with TBST, membranes were incubated with HRP-conjugated secondary antibodies for 30 min in 5% skimmed milk (Supplementary Table 2). Then, membranes were washed three times with TBST and bands visualized by enhanced chemiluminescence [36].

The evaluation of the phosphorylation status of multiple human kinases was carried out with the Proteome Profiler Human Phospho-Kinase Array Kit. In addition, the phosphorylation status of diverse RTKs was analyzed with the Proteome Profiler Human Phospho-RTK Array Kit (R&D Systems, Minneapolis, Minnesota, United States) following the manufacturer's instructions and as described [37]. For this, 300 μg of protein lysates from each cell line were hybridized with each membrane of the kit. The protein phosphorylation levels were quantified with Image Studio Lite Ver 5.2 (LI-COR, Lincoln, USA) and the values were represented as the mean pixel intensity of the duplicates for each protein. The intensity values of the negative controls were taken as background and only the values of phosphorylated proteins that exceeded this threshold value were represented.

2.7. EGFR and HER2 cell surface levels

Cytometric assessment of cell surface HER2 was performed by incubating cells with 10 nM of T-DM1 for 1 h [38]. The cell-bound antibodies were detected after an incubation with a Cy3-conjugated anti-human secondary antibody (1:80) for 30 min. To analyze EGFR cell surface levels, cells were incubated with Alexa 488-labelled cetuximab (1:1000) for 1 h. Mean fluorescence levels were determined using a BD Accuri C6 flow cytometer. For cell surface immunoprecipitation, cells were washed twice with Krebs-Ringer-HEPES buffer (KRH, 140 mM NaCl, 5 mM KCl, 2 mM $CaCl_2$, 5 mM $MgSO_4$, 1.2 mM KH_2PO_4, 6 mM glucose, 50 mM HEPES, pH 7.4) [36,39] and incubated in the KRH buffer with 10 nM T-DM1 or cetuximab for 2 h at 4 °C. Then, cells were lysed and cell-bound antibodies precipitated with protein A-Sepharose. Immunocomplexes were washed and HER2 or EGFR were detected by Western blotting.

2.8. Immunofluorescence (IF) and mitotic index

40,000 cells were cultured on glass coverslips and treated with 10 nM T-DM1 at the indicated times. Then, cells on coverslips were washed with PBS/CM (1 mM $CaCl_2$, 0.5 mM $MgCl_2$ in PBS) and fixed in 2% paraformaldehyde. After that, cells were washed in PBS/CM, quenched with 50 mM NH_4Cl and permeabilized (0.1% Triton, 0.2% BSA). Then, cells were incubated in blocking solution (PBS/CM with 0.2% BSA) for 1 h. Cells were washed in PBS/CM/BSA three times and then incubated with LAMP1 primary antibody and Cy2-conjugated anti-rabbit IgG

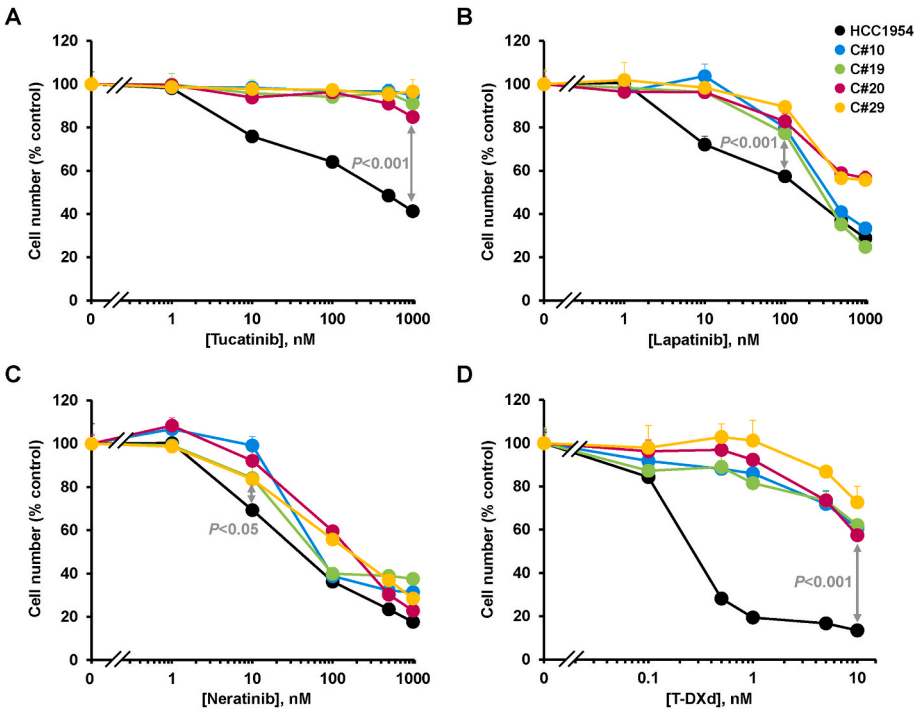

Fig. 3. Effect of different anti-HER2 approved therapies on the proliferation of the HCC1954 cell line and HCC-TDM1R clones. Dose-response analysis of the effect of (A) tucatinib (72h), (B) lapatinib (72h), (C) neratinib (72h) and (D) T-DXd (120h) on the proliferation of HCC1954 cells and T-DM1-resistant clones. Data represent mean +SD of triplicates (normalized to untreated controls) analyzed in a cell counting experiment that was repeated twice.

secondary antibody. To detect cetuximab-DM1, Cy3-conjugated anti-human IgG was used.

Mitotic cell number analysis was analyzed by immunofluorescence. Cells were cultured, treated with 10 nM cetuximab-DM1 for 48 h and processed as above. In this case, after blocking the samples, they were incubated with the anti-β-tubulin antibody for 1 h and then with the Cy2-conjugated anti-mouse secondary antibody. The samples were then observed on a Zeiss Axiophot 2 microscope with a 40x oil immersion objective. Twenty representative photos were taken for each condition. Among these cells, those with condensed chromosomes and a formed mitotic spindle were distinguished as mitotic cells, and those with condensed chromosomes but an abnormal mitotic spindle arrangement as aberrant mitotic cells. Finally, the percentage of mitotic cells with aberrant mitotic spindles was calculated as follows: Aberrant mitotic cells (%) = ((cells with aberrant mitotic spindle)/(total mitotic cells)) x 100. Represented photos of immunofluorescence experiments were taken by confocal IF microscopy using a Leica TCS SP5 system (Leica Microsystems CMS, Wetzlar, Germany).

2.9. Xenograft studies

Female BALB/c nu/nu mice were purchased from Charles River Laboratories and maintained at the animal facility of the University of Salamanca following legal and institutional guidelines. 4×10^6 HCC1954, HCCTDM1R#19 or HCCTDM1R#20 cells resuspended in DMEM and Matrigel (BD Biosciences) were injected orthotopically into the mammary fat pad, at two sites per mice. Animals (n = 4–5) with tumors of 200–300 mm^3 were randomized and intraperitoneally treated with vehicle alone (PBS), T-DM1 (15 mg/kg) or cetuximab-DM1 (15 mg/kg). Tumor volumes were measured with calipers and calculated by the following formula: volume = ($width^2 \times length$)/2. The percentage of relative tumor volume (RTV) was calculated using the following formula: RTV (%) = ((tumor volume on day 11)/(tumor volume on day 0)) x 100.

2.10. Statistical analyses

Data distributions were checked for normality by the Shapiro-Wilk test and homogeneity of variances was checked by the Levene test. One-way ANOVA followed by Games-Howell or Bonferroni post hoc was used to compare control group versus experimental groups. Statistical analyses were performed using SPSS 25 (SPSS Inc., Chicago, IL, USA).

3. Results

3.1. Generation of T-DM1-resistant breast cancer cells

We used the cell line HCC1954 to generate T-DM1-resistant models due to its primary resistance to trastuzumab [32]. The idea of using this cell line was to model the possible resistance generated in clinical practice, since patients treated with T-DM1 have previously been treated with trastuzumab-based therapies [13]. HCC1954 cells were treated with 1 nM T-DM1 for a total of 5 months and 25 clones were obtained (Fig. 1A). HCC-TDM1R#10, #19, #20 and #29 clones were selected for further analyses because they showed resistance to T-DM1 (Fig. 1B). All the selected clones preserved resistance to trastuzumab, in addition to acquired secondary resistance to T-DM1. All clones remained adherent to the culture substrate and their morphology was very similar to the HCC1954 parental cell line (Fig. 1C).

To explore whether the clones selected for T-DM1 resistance were different among them, transcriptomic profiling was made. Principal component analyses (PCA) of variance among the array data revealed clustering of the triplicates obtained from each cell line (Fig. 1D). Such clustering is suggestive of homogeneous gene expression profile of those samples within each clone. Furthermore, the different cell lines followed a different distribution in the three-dimensional (3D) representation of PCA, confirming substantial differences between the parental line HCC1954 and the HCC-TDM1R clones, and also between the different clones. Next, a comparative analysis of gene expression was carried out between the T-DM1-resistant clones and the HCC1954 cell line. This analysis revealed that all the clones expressed a considerable number of

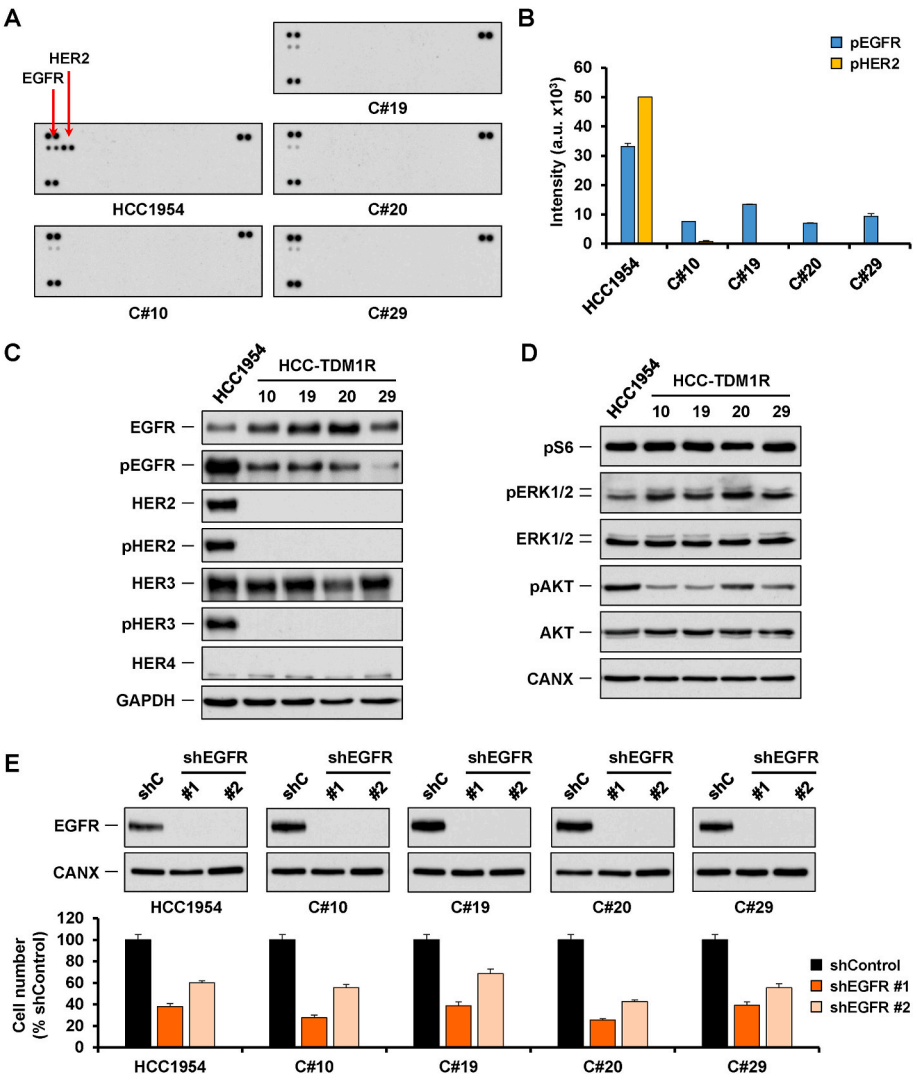

Fig. 4. Expression and role of EGFR on the proliferation of the HCC1954 cell line and HCC-TDM1R clones. (A) Evaluation of the basal levels of activation of different receptors by the phospho-RTK array kit. The protein extracts of the cell lines were incubated with the antibody membranes following the protocol of the commercial kit. The duplicate signals from the three corners are the positive controls for each membrane. (B) Quantitative representation of the pEGFR and pHER2 signals from the antibody array studies shown in A. a.u. = arbitrary units. A 50,000 arbitrary units value was assigned when the quantization of the signal was saturated. (C) Total and tyrosine phosphorylated ErbB receptor levels analyzed by immunoprecipitation in the HCC1954 cell line and T-DM1-resistant clones. GAPDH was used as a loading control. (D) Levels of pS6, pERK1/2, ERK1/2, pAKT and AKT in HCC1954 cells and T-DM1-resistant clones. (E) Knockdown of EGFR in HCC1954 cells and T-DM1-resistant clones. Cells were infected with lentivirus containing the shRNA control (shC, shControl) or the shRNA sequences targeting EGFR (shEGFR #1 y shEGFR #2). EGFR and CANX levels were analyzed by western (top). Effect of EGFR knockdown (bottom graphics) on the cell proliferation analyzed by cell counting after 5 days. Data are shown as mean +SD of triplicates of an experiment that was repeated three times.

differentially expressed genes (DEGs) compared to the parental line and compared between them (Fig. 1E). The analysis of the microarray data showed a lower expression of *ERBB2* in all HCC-TDM1R clones with respect to the parental line, being significant this difference in expression in all comparisons (Supplementary Fig. 1A).

3.2. T-DM1-resistant clones express low HER2 levels but remain addicted to HER2

ERBB2 downregulation was corroborated by qPCR in the T-DM1-resistant clones with respect to the parental cells (Fig. 2A). Moreover, when total HER2 levels were analyzed by western, all HCC-TDM1R clones showed substantially lower levels of HER2 when compared to the parental line HCC1954 (Fig. 2B). HER2 surface immunoprecipitation (Fig. 2C) and flow cytometry experiments (Fig. 2D) showed low HER2 levels in the HCC-TDM1R clones compared to the HCC1954 parental line. Immunofluorescent experiments confirmed low HER2 levels, both surface and total, in T-DM1-resistant cell lines (Fig. 2E). Reconstitution of human HER2 restored sensitivity to T-DM1 (Supplementary Figs. 1B and 1C).

To explore whether the remaining HER2 was able to promote the proliferation of the HCC-TDM1R clones, knock down experiments were carried out. HER2 silencing similarly affected the proliferation of the parental HCC1954 cell line and HCC-TDM1R clones (Fig. 2F).

3.3. HCC-TDM1R clones are less sensitive to other anti-HER2 therapies

The response to other anti-HER2 therapies approved in the clinic for the treatment of HER2+ breast cancer was tested. Tucatinib, a HER2 selective TKI [23,24], had no effect on HCC-TDM1R clones (Fig. 3A). Lapatinib, a TKI directed against HER2 and EGFR [18], was effective in all cell lines (Fig. 3B), as was neratinib (Fig. 3C), which is a pan-HER TKI [22]. However, the HCC-TDM1R clones showed lower sensitivity to neratinib and lapatinib compared to the parental line. The effect of the recently clinically approved ADC targeting HER2 T-DXd was also analyzed. The HCC-TDM1R clones were resistant to T-DXd while the parental line was sensitive (Fig. 3D).

3.4. Activated EGFR is expressed in HCC-TDM1R clones

To search for potential druggable targets that may be used to fight resistance to T-DM1 we analyzed the activation status of several receptor tyrosine kinases (RTKs) using antibody arrays. These RTK arrays allow analysis of the phosphorylation status of different RTKs some of them well known to act promoting cell proliferation and for which drugs have been developed. In addition, a second antibody array which analyzes the phosphorylation status of several signaling proteins involved in oncogenic processes was also used. These studies demonstrated that EGFR was phosphorylated in HCC-TDM1R clones and parental cells (Fig. 4A). However, the phosphorylation levels of the EGFR were higher

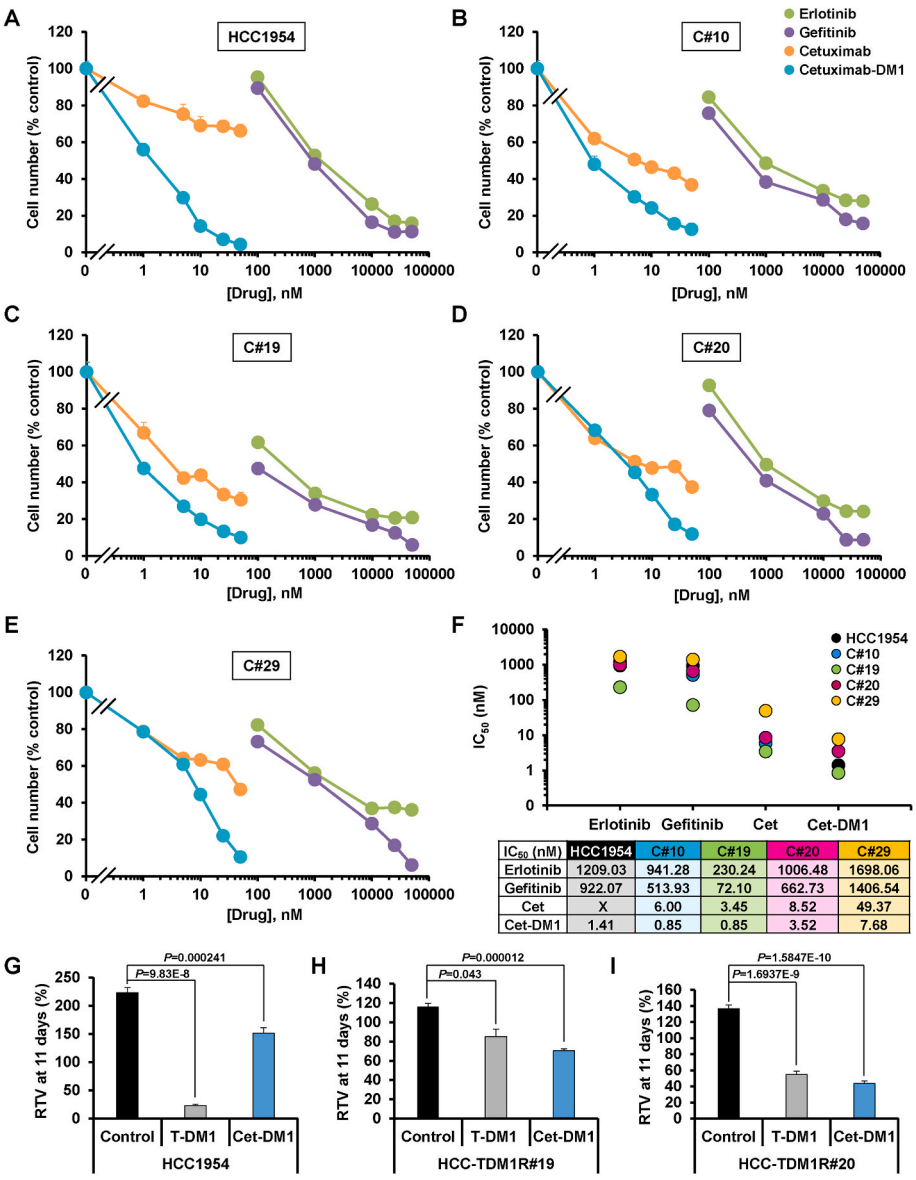

IC_{50} (nM)	HCC1954	C#10	C#19	C#20	C#29
Erlotinib	1209.03	941.28	230.24	1006.48	1698.06
Gefitinib	922.07	513.93	72.10	662.73	1406.54
Cet	X	6.00	3.45	8.52	49.37
Cet-DM1	1.41	0.85	0.85	3.52	7.68

Fig. 5. Effect of different therapies against EGFR on the proliferation of parental HCC1954 and HCC-TDM1R cells. (A–E) Dose-response analysis of the effect of erlotinib (72h), gefitinib (72h), cetuximab (120h) and cetuximab-DM1 (120h) on the proliferation of the indicated cell lines. Data represented as mean +SD of triplicates. (F) IC_{50} values for each drug and cell lines are represented in the graph (top) and detailed in the table (bottom). (G-I) *In vivo* effect of T-DM1 (15 mg/kg), cetuximab-DM1 (15 mg/kg) and vehicle (PBS) on tumor growth in mice injected with (G) HCC1954, (H) HCC-TDM1R#19 or (I) HCC-TDM1R#20 cells. Data are represented as mean +SEM. RTV: relative tumor volume. *P*-values are shown.

in the parental cells than in the resistant clones (Fig. 4B). The parental HCC1954 cell line also expressed active HER2, to levels above that of pEGFR. In contrast, the HCC-TDM1R clones did not show active HER2, as expected from their low expression levels.

In the second phospho-signaling array experimental setting, the activation status of most of the proteins analyzed was quite similar among all of them (Supplementary Fig. 2). The only proteins that showed greater phosphorylation in the HCC-TDM1R clones with respect to the parental cell line HCC1954 were c-Jun and p53.

Having observed the presence of phosphorylated EGFR in the resistant clones, the total levels of EGFR were analyzed by western. The level of EGFR was slightly higher in HCC-TDM1R clones with respect to the parental cell line (Fig. 4C). In agreement with the antibody array data, these studies confirmed that pEGFR levels were higher in parental HCC1954 than in the T-DM1-resistant clones (Fig. 4B and C). Cell-surface EGFR levels analyzed by either surface immunoprecipitation or flow cytometry were similar among the parental and the T-DM1-resistant clones (Supplementary Figs. 3A and 3B). These studies also indicated that the levels of the cognate ERBB family receptor HER3 were similar among all the analyzed cell lines. In the case of HER4, its levels were undetectable in these experiments. Since the EGFR appeared phosphorylated, the expression of its seven ligands was then explored. Quantitative PCR analyses showed different degrees of expression of all EGFR ligands in all the cell lines analyzed (Supplementary Fig. 3C). In addition, the expression levels and activation status of the main proteins involved in the signaling pathways were then analyzed by western studies. The levels of all of them were similar between the T-DM1-resistant clones and the parental cell line HCC1954, confirming no major changes in signaling pathways among cell lines (Fig. 4D).

3.5. *Targeting the EGFR in HCC-TDM1R clones*

To analyze the possible role of the EGFR in the proliferation of parental HCC1954 and HCC-TDM1R clones, we used genetic as well as pharmacological approaches. The genetic approach was based on the silencing of this RTK by shRNA sequences. In a previous report in which five different shRNA sequences were used, those ones that achieved the best knockdown levels were identified [40]. In the present knockdown studies, reduction of EGFR levels significantly inhibited the proliferation of HCC1954 cells and HCC-TDM1R clones (Fig. 4E).

Next, the effect of two clinically approved TKIs against EGFR, erlotinib and gefitinib, as well as the effect of cetuximab and an ADC derived

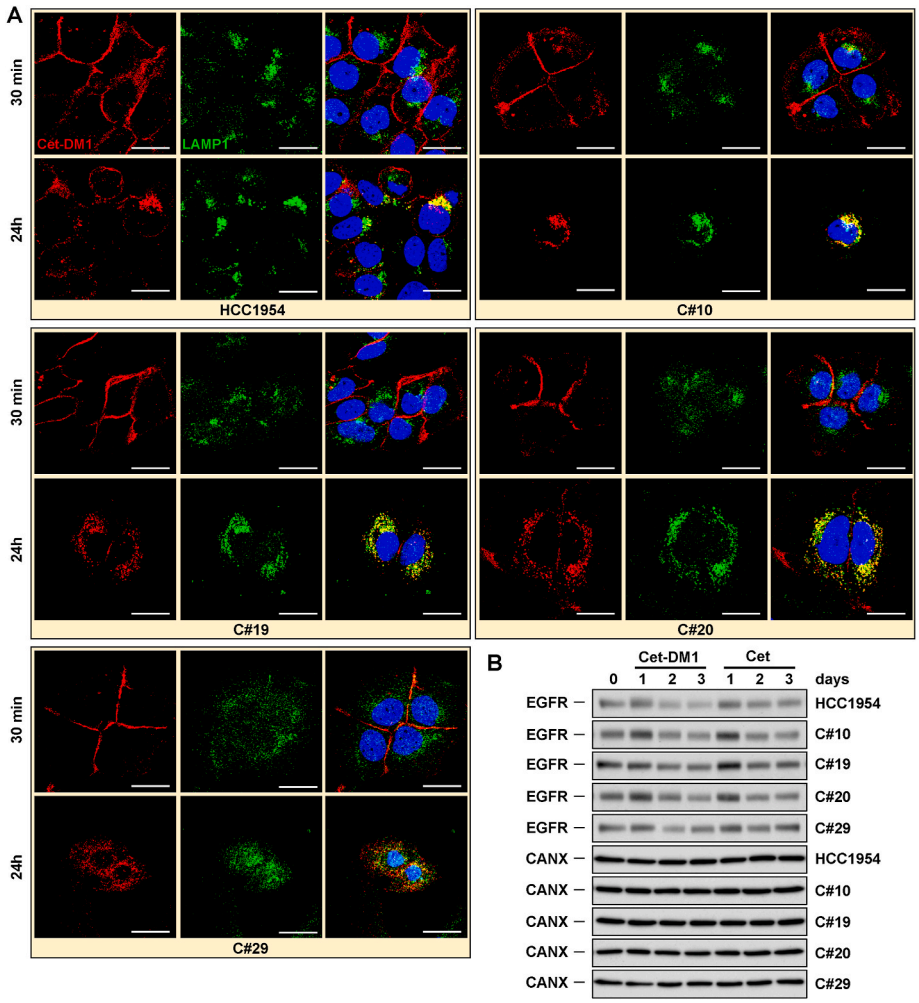

Fig. 6. Internalization of cetuximab-DM1 in HCC1954 cell line and HCC-TDM1R clones. (A) Colocalization (yellow) between cetuximab-DM1 (10 nM) and LAMP1 at the indicated incubation times in HCC1954 and HCC-TDM1R cells. Scale bar: 25 μm. Cetuximab-DM1 staining red, LAMP1: green, DAPI: blue. (B) Western blot analyses of the effect of cetuximab-DM1 (10 nM) and cetuximab (10 nM) on the EGFR levels in HCC1954 and HCC-TDM1R cells at the indicated incubation times with the antibodies.

from the latter were studied (Fig. 5). Both TKIs were effective in all cell lines, albeit at concentrations in the micromolar range. In the case of the humanized monoclonal antibody cetuximab, and in addition to using the nude antibody, we prepared an ADC version of cetuximab by its coupling to DM1. Western blotting analysis using an antibody raised against DM1 demonstrated the coupling of that payload to cetuximab (Supplementary Fig. 4).

As shown in Fig. 5, all lines were sensitive to cetuximab. Moreover, the antiproliferative effect of cetuximab-DM1 was in general more efficient and more potent than that observed with the nude antibody in all cell line analyzed. The action of cetuximab or cetuximab-DM1 was observed at nanomolar doses, demonstrating potency at concentrations several orders of magnitude below the TKIs. Indeed, cetuximab-DM1 had the lowest value of IC_{50} of all the treatments evaluated (Fig. 5F). Whether treatment with cetuximab-DM1 was effective *in vivo* was explored by orthotopically injecting HCC1954, HCC-TDM1R#19 or HCC-TDM1R#20 in mice. *In vivo*, cetuximab-DM1 significantly decreased tumor growth in HCC1954, HCC-TDM1R#19 and HCC-TDM1R#20 xenografts (Fig. 5G–I). These *in vivo* studies also demonstrated that T-DM1 was effective in tumors created by the injection of HCC1954 cells. In contrast, tumors created by injecting T-DM1-resistant clones, especially HCC-TDM1R#19 cells, were much more resistant to the antitumoral action of T-DM1, demonstrating that resistance to that drug is preserved in the *in vivo* environment. Of note, we observed that tumors created by injection of HCC-TDM1R#19 and HCC-TDM1R#20 cells grew slower than those created by injecting the parental cells.

3.6. Mechanism of action of Cetuximab-DM1

Immunofluorescence studies indicated that cetuximab-DM1 staining was restricted to the cell surface at an early incubation time (30 min, Fig. 6A). At 24 h, the staining evolved to a dotted pattern, suggesting the internalization of the antibody. Internalization of cetuximab-DM1 is expected to drive the ADC-EGFR complex to the lysosomes, where lysosomal proteolytic enzymes may cleave the ADC. Indeed, immunofluorescence experiments showed colocalization of cetuximab-DM1 with the lysosomal marker LAMP1. The same staining pattern was observed with the antibody cetuximab (Supplementary Fig. 5). Total EGFR levels were slightly downregulated by cetuximab and cetuximab-DM1 at 48 and 72 h (Fig. 6B).

To analyze the mechanism of the antitumoral action of cetuximab-DM1, the action of this compound on the cell cycle and cell viability/cell death were explored. Cetuximab-DM1 provoked accumulation of cells in G_2/M and a decrease in the G_0/G_1 cell cycle phases (Fig. 7A). Western blotting studies showed that the anti-EGFR ADC caused an accumulation of pHistone H3 and an increase in the levels of pBubR1, proteins that mark cells in mitosis (Fig. 7B).

The induction of mitotic arrest caused by certain cytotoxic payloads has been reported to provoke cell death through mitotic catastrophe due to alterations of microtubule polymerization during mitosis [31,41]. Cetuximab-DM1 affected the formation of normal mitotic spindles in all the cell lines analyzed (Fig. 7C and D). In the cultures treated with cetuximab-DM1, accumulation of non-viable cells was observed, as measured by annexin-V/propidium iodide staining (Fig. 7E). Treatment

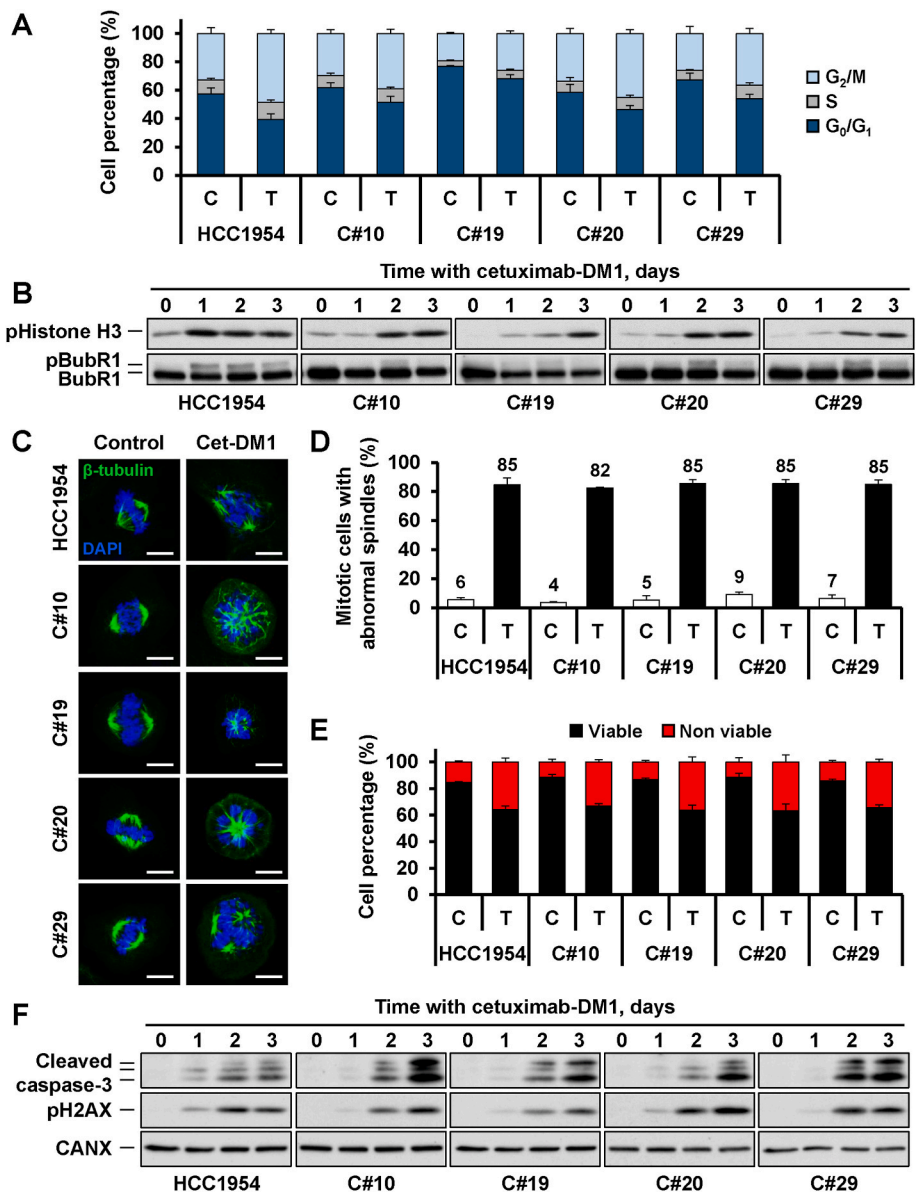

Fig. 7. Mechanism of action of cetuximab-DM1. (A) Cell cycle analysis by flow cytometry of HCC1954 and HCC-TDM1R clones treated with cetuximab-DM1 for 3 days. C: control, T: treated with 10 nM cetuximab-DM1. (B) Cells were treated for the indicated days with cetuximab-DM1 (10 nM) and pHistone H3 and BubR1 analyzed by Western. (C) Cells were treated with cetuximab-DM1 (10 nM, 48 h), fixed, and stained for β-tubulin (green) and DAPI (blue). Scale bar: 7.5 μm. (D) Quantitative analysis of mitotic cells with abnormal spindles treated or not with cetuximab-DM1 (10 nM, 48 h). Bars represent the mean +SD of three independent experiments, calculated as follows: ((number of mitotic cells with abnormal spindles)/(total number of mitotic cells)) × 100 (%). (E) Cell death induction was analyzed by double Annexin V and PI staining in HCC1954 cells and HCC-TDM1R clones treated or not with cetuximab-DM1 (10 nM, 72h). (F) Levels of cleaved caspase-3 and pH2AX analyzed by Western blotting in the indicated cell lines. CANX was used as a loading control.

with the ADC caused cleavage of caspase-3 and increased pH2AX in HCC1954 and HCC-TDM1R clones (Fig. 7F), indicative of induction of apoptosis and in line with the cell death observed.

HCC-TDM1R clones (C#10, C#19, C#20 and C#29) demonstrated their resistant phenotype to T-DM1 by failure of this ADC to (i) affect their proliferation (Supplementary Fig. 6A), (ii) cause mitotic arrest (Supplementary Fig. 6B) and (iii) provoke cell death (Supplementary Fig. 6C). T-DM1 increased the levels of pHistone H3, pBUBR1, cleaved caspase-3 and pH2AX in the parental cell line but not in the resistant clones (Supplementary Fig. 6D).

4. Discussion

To investigate resistance mechanisms against T-DM1 and strategies to overcome them, models of secondary resistance to T-DM1 were generated from the HER2+ cell line HCC1954. A common characteristic of the T-DM1-resistant clones was their substantial loss of HER2 expression. Since the target protein is critical in the mechanism of action of ADCs [31,41], it is likely that such loss is responsible for the resistance to T-DM1. In this respect, several reports have demonstrated that in patients with HER2+ breast cancer, partial or complete loss of HER2 represent mechanisms of resistance to anti-HER2 therapies [42–44]. Other studies have also shown changes in HER2 levels between primary tumors and breast cancer metastases, with loss of HER2 being more frequent [45–48]. Indeed, several authors have reported that prior treatment with trastuzumab (±pertuzumab) can decrease HER2 levels and therefore decrease the efficacy of treatment with T-DM1 [48,49]. In the secondary resistance models to T-DM1 derived from the HCC1954 cell line, HER2 loss caused cross-resistance to T-DXd. While the latter may retain some activity in HER2 low tumors [29], in the case of our T-DM1-resistant models it was unable to have an antitumoral effect. It is possible that the lack of action of T-DXd may derive from the lack of bystander action in cell models with homogeneous amount of low HER2. In line with our findings, T-DM1 has been shown to be ineffective in tumors with low levels of HER2 and/or heterogeneity in HER2 expression [50]. While the low level of HER2 may be responsible for the refractoriness of the T-DM1-resistant clones to the ADC, they were still oncogenically dependent from HER2, as supported by the knockdown experiments and by certain degree of sensitivity to the small molecule TKIs. The T-DM1-resistant models showed substantial resistance to tucatinib. However, they still responded to neratinib and lapatinib, even though the potency of these drugs was clearly compromised in the

resistant clones. Our data allow us to conclude that (i) HER2 overexpression appears to be critical for the action of ADCs targeting this receptor, (ii) low levels of HER2 may be sufficient to confer some degree of oncogenic dependence to HER2, and (iii) low HER2 tumors may still be sensitive to TKIs, although at higher concentrations than tumors overexpressing HER2.

Since the clinically available HER2 targeting alternatives resulted largely ineffective, we searched for new therapeutic targets to fight T-DM1 resistance. Protein arrays showed that EGFR was active in both HCC1954 cells and HCC-TDM1R clones. The role of EGFR in acquired resistance to T-DM1 has been analyzed by several authors who have found that T-DM1-resistant models had lower levels of HER2 and increased levels of EGFR [51–53]. The gene knockdown assays performed demonstrated the role of EGFR in the proliferation of the HCC1954 and HCC-TDM1R cell lines. Moreover, treatment with TKIs directed against EGFR and with cetuximab and cetuximab-DM1 showed to be effective in the HCC1954 cell line and the T-DM1-resistant clones. However, cetuximab-DM1 demonstrated to be the best therapeutic option in HCC-TDM1R clones, presenting the lowest IC_{50} values in comparison with the other tested treatments. EGFR resulted to be an excellent target in our models because it was increased in T-DM1-resistant clones, it is recognized by cetuximab-DM1 and its decrease reduces the proliferation of HCC-TDM1R clones. Indeed, cetuximab-DM1 improved the efficacy of cetuximab thanks to the ADC format. Immunofluorescence analyses indicated that cetuximab-DM1 was properly internalized and moved to lysosomes. The action of proteases in such organelle is expected to produce fragments of the ADC capable of being transported to cytosol, where the cytotoxic payload would impair microtubule polymerization. Due to this action, cetuximab-DM1 produced mitotic catastrophe, arrest in G_2/M cell cycle phase and cell death as occurs with other cytotoxic payloads [32,38,54,55].

In conclusion, in this work cell models of resistance to T-DM1 have been generated from a HER2+ cell line with primary resistance to trastuzumab [56]. The decrease in HER2 levels has been identified as the mechanism of resistance to the two clinically approved ADCs T-DM1 and T-DXd. In these resistance models, targeting EGFR with cetuximab-DM1 resulted in an antiproliferative effect *in vitro* and *in vivo*, opening the possibility of studying the antitumoral action of anti-EGFR ADCs in clinical trials in the setting of HER2-loss metastatic breast cancer [57–63].

Availability of data and materials

The data that support the findings of this study are available from the corresponding author upon reasonable request.

Consent for publication

All authors agreed on the manuscript.

Authorship contributions section

Lucía Gandullo-Sánchez: Formal analysis, Data curation, Visualization, Validation, Investigation, Methodology, Writing-review & editing, Writing-original draft. Atanasio Pandiella: Conceptualization, Project administration, Funding acquisition, Supervision, Resources, Writing-review & editing.

Declaration of competing interest

The authors declare that they have no known competing financial interests or personal relationships that could have appeared to influence the work reported in this paper.

Acknowledgments

AP: Ministry of Economy and Competitiveness of Spain (BFU2015-71371-R and PID2020-115605RB-I00), the Instituto de Salud Carlos III through CIBERONC, Junta de Castilla y León (CSI146P20), ALMOM, ACMUMA, UCCTA, the CRIS Cancer Foundation and the Regional Development Funding Program (FEDER) "A way to make Europe". LGS was recipient of a predoctoral contract (BES-2016-077748); and is at present contracted by the Cancer Research Foundation of the Salamanca University (FICUS). We thank Dr. Patricia Tomás-Martín for her participation in the generation of HCC-TDM1R clones.

Appendix A. Supplementary data

Supplementary data to this article can be found online at https://doi.org/10.1016/j.canlet.2022.216024.

References

[1] J.S. Ross, E.A. Slodkowska, W.F. Symmans, L. Pusztai, P.M. Ravdin, G. N. Hortobagyi, The HER-2 receptor and breast cancer: ten years of targeted anti–HER-2 therapy and personalized medicine, Oncol. 14 (2009) 320–368.
[2] D.J. Slamon, G.M. Clark, S.G. Wong, W.J. Levin, A. Ullrich, W.L. McGuire, Human breast cancer: correlation of relapse and survival with amplification of the HER-2/neu oncogene, Science 235 (1987) 177–182.
[3] E. Cocco, S. Lopez, A.D. Santin, M. Scaltriti, Prevalence and role of HER2 mutations in cancer, Pharmacol. Ther. 199 (2019) 188–196.
[4] P.P. Di Fiore, J.H. Pierce, M.H. Kraus, O. Segatto, C.R. King, S.A. Aaronson, erbB-2 is a potent oncogene when overexpressed in NIH/3T3 cells, Science 237 (1987) 178–182.
[5] C.L. Arteaga, M.X. Sliwkowski, C.K. Osborne, E.A. Perez, F. Puglisi, L. Gianni, Treatment of HER2-positive breast cancer: current status and future perspectives, Nat. Rev. Clin. Oncol. 9 (2011) 16–32.
[6] O. Martínez-Sáez, A. Prat, Current and future management of HER2-positive metastatic breast cancer, JCO Oncol Pract 17 (2021) 594–604.
[7] S.M. Swain, S.-B. Kim, J. Cortés, J. Ro, V. Semiglazov, M. Campone, E. Ciruelos, J.-M. Ferrero, A. Schneeweiss, A. Knott, Pertuzumab, trastuzumab, and docetaxel for HER2-positive metastatic breast cancer (CLEOPATRA study): overall survival results from a randomised, double-blind, placebo-controlled, phase 3 study, Lancet Oncol. 14 (2013) 461–471.
[8] J. Baselga, J. Cortés, S.B. Kim, S.A. Im, R. Hegg, Y.H. Im, L. Roman, J.L. Pedrini, T. Pienkowski, A. Knott, E. Clark, M.C. Benyunes, G. Ross, S.M. Swain, Pertuzumab plus trastuzumab plus docetaxel for metastatic breast cancer, N. Engl. J. Med. 366 (2012) 109–119.
[9] R.e. Nahta, F. Esteva, Trastuzumab: triumphs and tribulations, Oncogene 26 (2007) 3637–3643.
[10] D.J. Slamon, B. Leyland-Jones, S. Shak, H. Fuchs, V. Paton, A. Bajamonde, T. Fleming, W. Eiermann, J. Wolter, M. Pegram, Use of chemotherapy plus a monoclonal antibody against HER2 for metastatic breast cancer that overexpresses HER2, N. Engl. J. Med. 344 (2001) 783–792.
[11] H.S. Rugo, S.-A. Im, F. Cardoso, J. Cortés, G. Curigliano, A. Musolino, M.D. Pegram, G.S. Wright, C. Saura, S. Escrivá-de-Romaní, Efficacy of margetuximab vs trastuzumab in patients with pretreated ERBB2-positive advanced breast cancer: a phase 3 randomized clinical trial, JAMA Oncol. 7 (2021) 573–584.
[12] A. Markham, Margetuximab: first approval, Drugs 81 (2021) 599–604.
[13] L. Amiri-Kordestani, G.M. Blumenthal, Q.C. Xu, L. Zhang, S.W. Tang, L. Ha, W. C. Weinberg, B. Chi, R. Candau-Chacon, P. Hughes, A.M. Russell, S.P. Miksinski, X. H. Chen, W.D. McGuinn, T. Palmby, S.J. Schrieber, Q. Liu, J. Wang, P. Song, N. Mehrotra, L. Skarupa, K. Clouse, A. Al-Hakim, R. Sridhara, A. Ibrahim, R. Justice, R. Pazdur, P. Cortazar, FDA approval: ado-trastuzumab emtansine for the treatment of patients with HER2-positive metastatic breast cancer, Clin. Cancer Res. 20 (2014) 4436–4441.
[14] G. von Minckwitz, C.S. Huang, M.S. Mano, S. Loibl, E.P. Mamounas, M. Untch, N. Wolmark, P. Rastogi, A. Schneeweiss, A. Redondo, H.H. Fischer, W. Jacot, A. K. Conlin, C. Arce-Salinas, I.L. Wapnir, C. Jackisch, M.P. DiGiovanna, P. A. Fasching, J.P. Crown, P. Wülfing, Z. Shao, E. Rota Caremoli, H. Wu, L.H. Lam, D. Tesarowski, M. Smitt, H. Douthwaite, S.M. Singel, C.E. Geyer Jr., Trastuzumab emtansine for residual invasive HER2-positive breast cancer, N. Engl. J. Med. 380 (2019) 617–628.
[15] K. Shitara, E. Baba, K. Fujitani, E. Oki, S. Fujii, K. Yamaguchi, Discovery and development of trastuzumab deruxtecan and safety management for patients with HER2-positive gastric cancer, Gastric Cancer 24 (2021) 780–789.
[16] S. Modi, C. Saura, T. Yamashita, Y.H. Park, S.B. Kim, K. Tamura, F. Andre, H. Iwata, Y. Ito, J. Tsurutani, J. Sohn, N. Denduluri, C. Perrin, K. Aogi, E. Tokunaga, S.A. Im, K.S. Lee, S.A. Hurvitz, J. Cortes, C. Lee, S. Chen, L. Zhang, J. Shahidi, A. Yver, I. Krop, Trastuzumab deruxtecan in previously treated HER2-positive breast cancer, N. Engl. J. Med. 382 (2020) 610–621.
[17] S.J. Keam, Trastuzumab deruxtecan: first approval, Drugs 80 (2020) 501–508.

[18] C.E. Geyer, J. Forster, D. Lindquist, S. Chan, C.G. Romieu, T. Pienkowski, A. Jagiello-Gruszfeld, J. Crown, A. Chan, B. Kaufman, Lapatinib plus capecitabine for HER2-positive advanced breast cancer, N. Engl. J. Med. 355 (2006) 2733–2743.
[19] K.L. Blackwell, H.J. Burstein, A.M. Storniolo, H.S. Rugo, G. Sledge, G. Aktan, C. Ellis, A. Florance, S. Vukelja, J. Bischoff, Overall survival benefit with lapatinib in combination with trastuzumab for patients with human epidermal growth factor receptor 2–positive metastatic breast cancer: final results from the EGF104900 study, J. Clin. Oncol. 30 (2012) 2585–2592.
[20] A. Chan, S. Delaloge, F.A. Holmes, B. Moy, H. Iwata, V.J. Harvey, N.J. Robert, T. Silovski, E. Gokmen, G. von Minckwitz, B. Ejlertsen, S.K.L. Chia, J. Mansi, C. H. Barrios, M. Gnant, M. Buyse, I. Gore, J. Smith 2nd, G. Harker, N. Masuda, K. Petrakova, A.G. Zotano, N. Iannotti, G. Rodriguez, P. Tassone, A. Wong, R. Bryce, Y. Ye, B. Yao, M. Martin, Neratinib after trastuzumab-based adjuvant therapy in patients with HER2-positive breast cancer (ExteNET): a multicentre, randomised, double-blind, placebo-controlled, phase 3 trial, Lancet Oncol. 17 (2016) 367–377.
[21] M. Martin, F.A. Holmes, B. Ejlertsen, S. Delaloge, B. Moy, H. Iwata, G. von Minckwitz, S.K.L. Chia, J. Mansi, C.H. Barrios, M. Gnant, Z. Tomašević, N. Denduluri, R. Šeparović, E. Gokmen, A. Bashford, M. Ruiz Borrego, S.B. Kim, E. H. Jakobsen, A. Ciceniene, K. Inoue, F. Overkamp, J.B. Heijns, A.C. Armstrong, J. S. Link, A.A. Joy, R. Bryce, A. Wong, S. Moran, B. Yao, F. Xu, A. Auerbach, M. Buyse, A. Chan, Neratinib after trastuzumab-based adjuvant therapy in HER2-positive breast cancer (ExteNET): 5-year analysis of a randomised, double-blind, placebo-controlled, phase 3 trial, Lancet Oncol. 18 (2017) 1688–1700.
[22] E.D. Deeks, Neratinib: first global approval, Drugs 77 (2017) 1695–1704.
[23] A. Lee, Tucatinib: first approval, Drugs 80 (2020) 1033–1038.
[24] R.K. Murthy, S. Loi, A. Okines, E. Paplomata, E. Hamilton, S.A. Hurvitz, N.U. Lin, V. Borges, V. Abramson, C. Anders, Tucatinib, trastuzumab, and capecitabine for HER2-positive metastatic breast cancer, N. Engl. J. Med. 382 (2020) 597–609.
[25] C. Vernieri, M. Milano, M. Brambilla, A. Mennitto, C. Maggi, M.S. Cona, M. Prisciandaro, C. Fabbroni, L. Celio, G. Mariani, G.V. Bianchi, G. Capri, F. de Braud, Resistance mechanisms to anti-HER2 therapies in HER2-positive breast cancer: current knowledge, new research directions and therapeutic perspectives, Crit. Rev. Oncol. Hematol. 139 (2019) 53–66.
[26] H. Sung, J. Ferlay, R.L. Siegel, M. Laversanne, I. Soerjomataram, A. Jemal, F. Bray, Global cancer statistics 2020: GLOBOCAN estimates of incidence and mortality worldwide for 36 cancers in 185 countries, CA Cancer J. Clin. 71 (3) (2021) 209–249.
[27] G.D.L. Phillips, G. Li, D.L. Dugger, L.M. Crocker, K.L. Parsons, E. Mai, W.A. Blättler, J.M. Lambert, R.V. Chari, R.J. Lutz, Targeting HER2-positive breast cancer with trastuzumab-DM1, an antibody–cytotoxic drug conjugate, Cancer Res. 68 (2008) 9280–9290.
[28] F.W. Hunter, H.R. Barker, B. Lipert, F. Rothé, G. Gebhart, M.J. Piccart-Gebhart, C. Sotiriou, S.M. Jamieson, Mechanisms of resistance to trastuzumab emtansine (T-DM1) in HER2-positive breast cancer, Br. J. Cancer 122 (2020) 603–612.
[29] E. Díaz-Rodríguez, L. Gandullo-Sánchez, A. Ocaña, A. Pandiella, Novel ADCs and strategies to overcome resistance to anti-HER2 ADCs, Cancers 14 (2021).
[30] M. Sánchez-Martín, A. Pandiella, Differential action of small molecule HER kinase inhibitors on receptor heterodimerization: therapeutic implications, Int. J. Cancer 131 (2012) 244–252.
[31] L. Gandullo-Sánchez, A. Ocaña, A. Pandiella, Generation of antibody-drug conjugate resistant models, Cancers 13 (2021).
[32] L. Gandullo-Sánchez, E. Capone, A. Ocana, S. Iacobelli, G. Sala, A. Pandiella, HER3 targeting with an antibody-drug conjugate bypasses resistance to anti-HER2 therapies, EMBO Mol. Med. 12 (2020), e11498.
[33] C. Ríos-Luci, E. Díaz-Rodríguez, L. Gandullo-Sánchez, L. Díaz-Gil, A. Ocaña, A. Pandiella, Adaptive resistance to trastuzumab impairs response to neratinib and lapatinib through deregulation of cell death mechanisms, Cancer Lett. 470 (2020) 161–169.
[34] A. Esparís-Ogando, A. Ocaña, R. Rodríguez-Barrueco, L. Ferreira, J. Borges, A. Pandiella, Synergic antitumoral effect of an IGF-IR inhibitor and trastuzumab on HER2-overexpressing breast cancer cells, Ann. Oncol. 19 (2008) 1860–1869.
[35] S. Seoane, J.C. Montero, A. Ocaña, A. Pandiella, Effect of multikinase inhibitors on caspase-independent cell death and DNA damage in HER2-overexpressing breast cancer cells, J. Natl. Cancer Inst. 102 (2010) 1432–1446.
[36] N. Cabrera, E. Díaz-Rodríguez, E. Becker, D. Martín-Zanca, A. Pandiella, TrkA receptor ectodomain cleavage generates a tyrosine-phosphorylated cell-associated fragment, J. Cell Biol. 132 (1996) 427–436.
[37] J.C. Montero, A. Esparis-Ogando, M.F. Re-Louhau, S. Seoane, M. Abad, R. Calero, A. Ocana, A. Pandiella, Active kinase profiling, genetic and pharmacological data define mTOR as an important common target in triple-negative breast cancer, Oncogene 33 (2014) 148–156.
[38] C. Ríos-Luci, S. García-Alonso, E. Díaz-Rodríguez, M. Nadal-Serrano, J. Arribas, A. Ocaña, A. Pandiella, Resistance to the antibody–drug conjugate T-DM1 is based in a reduction in lysosomal proteolytic activity, Cancer Res. 77 (2017) 4639–4651.
[39] E. Diaz-Rodriguez, N. Cabrera, A. Esparis-Ogando, J.C. Montero, A. Pandiella, Cleavage of the TrkA neurotrophin receptor by multiple metalloproteases generates signalling-competent truncated forms, Eur. J. Neurosci. 11 (1999) 1421–1430.
[40] S. García-Alonso, I. Romero-Pérez, L. Gandullo-Sánchez, L. Chinchilla, A. Ocaña, J. C. Montero, A. Pandiella, Altered proTGFα/cleaved TGFα ratios offer new therapeutic strategies in renal carcinoma, J. Exp. Clin. Cancer Res. 40 (2021) 256.
[41] S. García-Alonso, A. Ocaña, A. Pandiella, Resistance to antibody-drug conjugates, Cancer Res. 78 (2018) 2159–2165.
[42] V. Guarneri, M.V. Dieci, E. Barbieri, F. Piacentini, C. Omarini, G. Ficarra, S. Bettelli, P.F. Conte, Loss of HER2 positivity and prognosis after neoadjuvant therapy in HER2-positive breast cancer patients, Ann. Oncol. 24 (2013) 2990–2994.
[43] G. Bon, L. Pizzuti, V. Laquintana, R. Loria, M. Porru, C. Marchiò, E. Krasniqi, M. Barba, M. Maugeri-Saccà, T. Gamucci, R. Berardi, L. Livi, C. Ficorella, C. Natoli, E. Cortesi, D. Generali, N. La Verde, A. Cassano, E. Bria, L. Moscetti, A. Michelotti, V. Adamo, C. Zamagni, G. Tonini, G. Barchiesi, M. Mazzotta, D. Marinelli, S. Tomao, P. Marchetti, M.R. Valerio, R. Mirabelli, A. Russo, M.A. Fabbri, N. D'Ostilio, E. Veltri, D. Corsi, O. Garrone, I. Paris, G. Sarobba, F. Giotta, C. Garufi, M. Cazzaniga, P. Del Medico, M. Roselli, G. Sanguineti, I. Sperduti, A. Sapino, R. De Maria, C. Leonetti, A. Di Leo, G. Ciliberto, R. Falcioni, P. Vici, Loss of HER2 and decreased T-DM1 efficacy in HER2 positive advanced breast cancer treated with dual HER2 blockade: the SePHER Study, J. Exp. Clin. Cancer Res. 39 (2020) 279.
[44] E.A. Mittendorf, Y. Wu, M. Scaltriti, F. Meric-Bernstam, K.K. Hunt, S. Dawood, F. J. Esteva, A.U. Buzdar, H. Chen, S. Eksambi, G.N. Hortobagyi, J. Baselga, A. M. Gonzalez-Angulo, Loss of HER2 amplification following trastuzumab-based neoadjuvant systemic therapy and survival outcomes, Clin. Cancer Res. 15 (2009) 7381–7388.
[45] W. Schrijver, K.P.M. Suijkerbuijk, C.H. van Gils, E. van der Wall, C.B. Moelans, P. J. van Diest, Receptor conversion in distant breast cancer metastases: a systematic review and meta-analysis, J. Natl. Cancer Inst. 110 (2018) 568–580.
[46] G. Aurilio, D. Disalvatore, G. Pruneri, V. Bagnardi, G. Viale, G. Curigliano, L. Adamoli, E. Munzone, A. Sciandivasci, F. De Vita, A. Goldhirsch, F. Nolè, A meta-analysis of oestrogen receptor, progesterone receptor and human epidermal growth factor receptor 2 discordance between primary breast cancer and metastases, Eur. J. Cancer 50 (2014) 277–289.
[47] N. Niikura, J. Liu, N. Hayashi, E.A. Mittendorf, Y. Gong, S.L. Palla, Y. Tokuda, A. M. Gonzalez-Angulo, G.N. Hortobagyi, N.T. Ueno, Loss of human epidermal growth factor receptor 2 (HER2) expression in metastatic sites of HER2-overexpressing primary breast tumors, J. Clin. Oncol. 30 (2012) 593–599.
[48] E. Van Raemdonck, G. Floris, P. Berteloot, A. Laenen, I. Vergote, H. Wildiers, K. Punie, P. Neven, Efficacy of anti-HER2 therapy in metastatic breast cancer by discordance of HER2 expression between primary and metastatic breast cancer, Breast Cancer Res. Treat. 185 (2021) 183–194.
[49] S. Seo, M.H. Ryu, Y.S. Park, J.Y. Ahn, Y. Park, S.R. Park, B.Y. Ryoo, G.H. Lee, H. Y. Jung, Y.K. Kang, Loss of HER2 positivity after anti-HER2 chemotherapy in HER2-positive gastric cancer patients: results of the GASTric cancer HER2 reassessment study 3 (GASTHER3), Gastric Cancer 22 (2019) 527–535.
[50] A. Ocaña, E. Amir, A. Pandiella, HER2 heterogeneity and resistance to anti-HER2 antibody-drug conjugates, Breast Cancer Res. 22 (2020) 15.
[51] G. Li, J. Guo, B.-Q. Shen, D.B. Yadav, M.X. Sliwkowski, L.M. Crocker, J.A. Lacap, G. D.L. Phillips, Mechanisms of acquired resistance to trastuzumab emtansine in breast cancer cells, Mol. Cancer Therapeut. 17 (2018) 1441–1453.
[52] V. Le Joncour, A. Martins, M. Puhka, J. Isola, M. Salmikangas, P. Laakkonen, H. Joensuu, M. Barok, A novel anti-HER2 antibody-drug conjugate XMT-1522 for HER2-positive breast and gastric cancers resistant to trastuzumab emtansine, Mol. Cancer Therapeut. 18 (2019) 1721–1730.
[53] Y. Endo, Y. Shen, L.A. Youssef, N. Mohan, W.J. Wu, T-DM1-resistant cells gain high invasive activity via EGFR and integrin cooperated pathways, mAbs 10 (2018) 1003–1017.
[54] J.C. Montero, S. García-Alonso, A. Ocaña, A. Pandiella, Identification of therapeutic targets in ovarian cancer through active tyrosine kinase profiling, Oncotarget 6 (2015) 30057–30071.
[55] S. Garcia-Alonso, A. Ocana, A. Pandiella, Trastuzumab emtansine: mechanisms of action and resistance, clinical progress, and beyond, Trends Cancer 6 (2020) 130–146.
[56] E. Diaz-Rodriguez, J. Perez-Pena, C. Rios-Luci, J. Arribas, A. Ocana, A. Pandiella, TRAIL receptor activation overcomes resistance to trastuzumab in HER2 positive breast cancer cells, Cancer Lett. 453 (2019) 34–44.
[57] A.C. Phillips, E.R. Boghaert, K.S. Vaidya, M.J. Mitten, S. Norvell, H.D. Falls, P. J. DeVries, D. Cheng, J.A. Meulbroek, F.G. Buchanan, L.M. McKay, N.C. Goodwin, E.B. Reilly, ABT-414, an antibody–drug conjugate targeting a tumor-selective EGFR epitope, Mol. Cancer Therapeut. 15 (2016) 661–669.
[58] G.D. Goss, E.E. Vokes, M.S. Gordon, L. Gandhi, K.P. Papadopoulos, D.W. Rasco, J. S. Fischer, K.L. Chu, W.W. Ames, R.K. Mittapalli, H.J. Lee, J. Zeng, L.A. Roberts-Rapp, L.I. Loberg, P.J. Ansell, E.B. Reilly, C.J. Ocampo, K.D. Holen, A.W. Tolcher, Efficacy and safety results of depatuxizumab mafodotin (ABT-414) in patients with advanced solid tumors likely to overexpress epidermal growth factor receptor, Cancer 124 (2018) 2174–2183.
[59] J.J. Zoeller, A. Vagodny, V.W. Daniels, K. Taneja, B.Y. Tan, Y.S. DeRose, M. Fujita, A.L. Welm, A. Letai, J.D. Leverson, V. Blot, R.T. Bronson, D.A. Dillon, J.S. Brugge, Navitoclax enhances the effectiveness of EGFR-targeted antibody-drug conjugates in PDX models of EGFR-expressing triple-negative breast cancer, Breast Cancer Res. 22 (2020) 132.
[60] B.A. Carneiro, C.M. Bestvina, E.S. Shmueli, H.K. Gan, J.T. Beck, R. Robinson, J. S. Fischer, A. Wong, P.J. Ansell, J.Y. Jin, L. Naumovski, K.P. Papadopoulos, Phase I study of the antibody-drug conjugate ABBV-321 in patients with non-small cell lung cancer and squamous head and neck cancer with overexpression of the epidermal growth factor receptor, J. Clin. Oncol. 38 (2020). TPS3649-TPS3649.

[61] M. O'Connor-McCourt, J. Koropatnick, S. Maleki, R. Figueredo, I. Tikhomirov, M. Jaramillo, Development of AVID100, a novel antibody–drug conjugate for the treatment of EGFR expressing solid tumors, Eur. J. Cancer 69 (2016) S147.
[62] A. Tolcher, K. Papadopoulos, Y. Cole, K. Rivas, S. Chandana, S. Sinclair, D. Wood, P.I. Nadler, N. Lakhani, A Phase 1a/2a trial of AVID100, an anti-EGFR antibody-drug conjugate, Ann. Oncol. 29 (2018) iii8.
[63] R.-h. Xu, M.-Z. Qiu, Y. Zhang, X.-L. Wei, C. Hu, First-in-human dose-escalation study of anti-EGFR ADC MRG003 in patients with relapsed/refractory solid tumors, J. Clin. Oncol. 38 (2020), 3550-3550.